

Cite this: *Sustainable Food Technol.*,  
2024, 2, 1724

# Poly( $\epsilon$ -caprolactone) nanofibers functionalized with poultry feather hydrolysate as a novel antioxidant material†

Flávio Fonseca Veras, Naiara Jacinta Clerici, Aline Aniele Vencato  
and Adriano Brandelli \*

Bioactive keratin hydrolysates obtained from microbial treatment of poultry feathers were incorporated into polycaprolactone (PCL) nanofibers using the electrospinning method. The nanofiber mats were characterized by scanning electron microscopy (SEM), Fourier transform infrared (FTIR) spectroscopy, thermal analysis, and hemolysis rate. Feather keratin hydrolysate (FKH) was effectively incorporated into the nanofibers, and the antioxidant activity of the nanomaterials was confirmed. The SEM analysis revealed the formation of fibers with typical string-like morphology and nanometric size. The average diameter of nanofibers containing 1, 2.5 and 5% FKH was 348, 363 and 533 nm, respectively. FTIR spectra showed no relevant interactions between the hydrolysate and the polymer during the electrospinning process, and the FKH addition caused no important modifications on the thermal properties of the nanofibers such as thermal degradation rate, melting temperature, and crystallinity, which were investigated using TGA and DSC techniques. Furthermore, the functionalized nanofibers showed low hemolysis rates (up to 3%) suggesting they are safe materials when considering the acceptable hemolysis threshold for biocompatible materials (below 5%). Preliminary tests revealed that FKH can be released from the nanofibers in food simulant solutions. Considering these results, the electrospun PCL nanofibers are promising candidates for incorporation of bioactive feather hydrolysates with potential application as food packaging materials.

Received 22nd August 2024  
Accepted 11th September 2024

DOI: 10.1039/d4fb00250d

rsc.li/susfoodtech

## Sustainability spotlight

Research involving biotechnological processes and nanotechnology contributes considerably to the reuse of agro-industrial waste, generating valued products and reducing the environmental impact. In particular, poultry production is notable for its annual growth and consequent generation of waste. The development of novel nanomaterials with antioxidant properties for food packaging applications could contribute to the proper management and recycling of such residues generated in huge amounts by the food industry.

## 1 Introduction

Industrial waste coming from poultry production, consisting mainly of feathers, becomes a risk to the environment when not disposed of properly. An estimated 8 to 10 million tons of feathers are produced annually by poultry farming, which emphasizes the need to take action to reduce or prevent its environmental accumulation.<sup>1,2</sup> Therefore, the reuse of this waste to develop new materials with environmentally sustainable applications should be encouraged. Such action is recognized as an alternative to reduce negative impacts on the

environment, in addition to adding value to this byproduct.<sup>2-4</sup> One of the crucial aspects of enabling the sustainable reuse of feather waste is to explore the intrinsic properties of these materials, as well as their possibilities for modification for specific applications. In this context, the keratin present in feathers plays a central role in this process.

Keratin is the main component of feathers, one of the most abundant proteins of animal origin, widely known for its structural rigidity and low solubility.<sup>5</sup> However, investigations on the use of microorganisms as a possible sustainable strategy for managing feather waste reported that enzymatic hydrolysis can modify the functional properties of feather keratin, including its solubility.<sup>2,5</sup> Such protein hydrolysate may also contain bioactive peptides that are released through this enzymatic process, in addition to being considered safe since it presents good compatibility with biological systems.<sup>6,7</sup> In particular, *Chryseobacterium* sp. kr6, isolated from poultry

Laboratório de Nanobiotecnologia e Microbiologia Aplicada, Instituto de Ciência e Tecnologia de Alimentos, Universidade Federal do Rio Grande do Sul, 91501-970 Porto Alegre, Brazil. E-mail: [abrand@ufrgs.br](mailto:abrand@ufrgs.br)

† Electronic supplementary information (ESI) available. See DOI: <https://doi.org/10.1039/d4fb00250d>



industry effluents, has been noted for its greater efficiency in the bioconversion of feathers compared to widely recognized feather-degrading bacterial strains.<sup>8</sup> This effect occurs due to the kr6 strain's ability to produce four extracellular proteases: two are broadly substrate-specific and the remaining two are produced exclusively in the presence of feathers.<sup>8,9</sup> The feather hydrolysate obtained by the action of this strain has shown biological activities, such as antihypertensive (angiotensin converting enzyme-I inhibition), antidiabetogenic (dipeptidyl-peptidase IV inhibition) and mainly antioxidant properties, indicating its potential for biotechnological applications.<sup>9–11</sup>

Among other approaches for reusing agro-industrial waste, nanotechnology has experienced exponential growth in recent years. In this area of research, the different properties of the materials developed (for example, nanofibers, nanoparticles, nanocapsules, among others) allow the obtaining of new functionalities for countless applications, contributing to significant advances mainly in the fields of medicine, physics, biology, chemistry and engineering.<sup>12–14</sup> A specific example of innovation within nanotechnology is the production of nanofibers, which are fibrous structures with diameters on a nanometric scale, characterized by a high surface-to-volume ratio and obtained from different techniques chosen according to the desired properties and applications.<sup>13,15</sup>

Nanofibers made by the electrospinning technique stand out from other nanostructures due to the simplicity and low production cost, as well as the ability to incorporate different compounds, acquiring specific functionality corresponding to the added substance.<sup>15,16</sup> This technique is an effective way to produce nanofibers, which can provide controlled release of various compounds, such as proteins, drugs or active agents.<sup>17–20</sup> Various organic or inorganic materials, in addition to polymeric mixtures, can compose the nanofiber matrix. Poly- $\epsilon$ -caprolactone (PCL), for example, is a synthetic, biodegradable and low-toxic polymer, which has been considered favorable for the manufacture of these nanostructures.<sup>17,21–23</sup> Notably, the biodegradation capacity of PCL is considered the main advantage for its use, given the possibility of replacing the traditional synthetic polymers.<sup>24</sup> Due to the non-biodegradable nature of these polymers, their persistent accumulation in soil and water bodies negatively affects ecosystems.<sup>25</sup> In this scenario, PCL has been reported as a promising alternative in the industry, including in the food packaging sector, owing to the demand for sustainable materials or those with lower environmental impact.<sup>26</sup> Furthermore, attributes such as good processability and compatibility of PCL with other polymers also contribute to its use in the development of packaging systems, especially those with active technologies and thus, maintaining the physicochemical and sensory characteristics of food products to extend their shelf life.<sup>24,26</sup>

Different approaches have been developed to produce PCL nanofibers with biofunctional properties.<sup>17,27,28</sup> Research on the fabrication of PCL-based nanofibers functionalized with antioxidant compounds has been conducted lately, demonstrating their potential for use in biomedical and pharmaceutical applications, and active food packaging as well.<sup>28–31</sup> In this latter case, there is an efficient interaction between the food, the

packaging material and the environment, reducing oxidation reactions involved in food spoilage, thus preserving food quality and sensory properties.<sup>24,32,33</sup> As the electrospinning process allows the incorporation of various compounds into the nanofibers, the bioactive peptides released during the conversion of keratin by *Chryseobacterium* sp. kr6 could provide antioxidant properties to the resulting fibers, making them potentially applicable in the food industry. In this regard, the use of feather keratin hydrolysates for the development of polymeric films by electrospinning has not been previously reported. Research into the use of feather hydrolysate to produce a new nanomaterial for food packaging could offer a number of benefits compared to other bioactive substances, including sustainability issues and production costs. The presence of specific bioactive peptides, which influence biological processes in unique ways, in addition to their thermal stability, biocompatibility and safety for use in food must also be considered.

This study aimed to investigate the potential of feather keratin hydrolysate produced from *Chryseobacterium* sp. kr6 for preparing PCL nanofiber films with antioxidant properties. The morphology, structure, thermal properties, and hemocompatibility of these nanostructures were also evaluated. Finally, the nanofibers were investigated about the hydrolysate release capacity into food simulants.

## 2 Materials and methods

### 2.1. Chemicals

Poly- $\epsilon$ -caprolactone (PCL; average MW 80,000), 2,2-diphenyl-1-picrylhydrazyl (DPPH), 2,2'-azino-bis-(3-ethylbenzothiazoline)-6-sulfonic acid (ABTS), and 6-hydroxy-2,5,7,8-tetramethylchroman-2-carboxylic acid (Trolox) were obtained from Sigma-Aldrich (St. Louis, MO, USA). Tetrahydrofuran (THF) and *N,N*-dimethyl formamide (DMF) were purchased from Merck (Darmstadt, Germany). Sodium chloride (NaCl), monopotassium phosphate (KH<sub>2</sub>PO<sub>4</sub>), and calcium chloride (CaCl<sub>2</sub>) were acquired from Labsynth (São Paulo, Brazil).

### 2.2. Microorganism

The keratinolytic bacterium *Chryseobacterium* sp. kr6, isolated from a poultry processing plant,<sup>34</sup> was used for production of feather hydrolysate. The strain was retrieved from the culture collection of the Laboratory of Applied Microbiology and Biochemistry (ICTA, UFRGS, Porto Alegre, Brazil). This strain was stored on Brain Heart Infusion (BHI; Oxoid, Basingstoke, UK) agar plates at 4 °C or for long term storage at –20 °C in BHI broth with 20% (v/v) glycerol and routinely propagated twice from frozen stocks before use.

### 2.3. Production of feather hydrolysate

Feathers were provided by a local poultry industry (Porto Alegre, RS, Brazil) and subjected to washing in running water and removal of impurities (nails, blood and pieces of skin), followed by rinsing in distilled water (3×). The material was subjected to drying in an oven at 45 °C and kept refrigerated until used for microbial treatment.<sup>34</sup> Feather keratin hydrolysate (FKH)



production was carried out through cultivation of the strain kr6 in a medium composed of 5 g L<sup>-1</sup> of whole chicken feathers, 0.5 g L<sup>-1</sup> NaCl, 0.4 g L<sup>-1</sup> KH<sub>2</sub>PO<sub>4</sub>, and 0.15 g L<sup>-1</sup> CaCl<sub>2</sub>, previously sterilized. The bacterial cultivation was performed at 30 °C with continuous shaking (125 rpm) for 48 h. After growth, bacterial cells were removed by centrifugation at 10 000g for 15 min at 4 °C. The crude hydrolysate was treated by autoclaving (121 °C, 20 min), followed by lyophilization in a freeze dryer (FreeZone 6, Labconco Co.) at -45 °C under a pressure of 13.3 Pa for 48 h. The product was sealed and stored in a freezer at -20 °C until further utilization.<sup>9</sup> The hydrolysis was confirmed by soluble protein content determination (1.8 mg mL<sup>-1</sup>) and DPPH and ABTS radical scavenging assays (28.6%; 181 μM TEAC and 36.7%; 721 μM TEAC, respectively) from the culture supernatant before lyophilization as described previously.<sup>10</sup>

#### 2.4. Preparation of nanofibers by electrospinning

Electrospinning solution (10 wt% PCL) was prepared by dissolving 2.5 g of PCL powder in 25 mL of THF : DMF (1 : 1, v/v) solution and stirred for 1 h at room temperature until a clear solution was obtained. Subsequently, different concentrations of the hydrolysate (1, 2.5 and 5% in relation to the polymer) were added to the polymer solution and mixed homogeneously using a magnetic stirrer at room temperature for 16 h before electrospinning. PCL solution without the FKH solution was prepared as a control in order to produce the control nanofibers.

The polymeric solutions were placed in a plastic syringe fitted with a metallic needle of 0.5 mm inner diameter and subjected to electrospinning as described by Veras *et al.*,<sup>35</sup> with some modifications. The process was conducted under the following conditions: 3 mL polymer injected volume, 30 kV voltage, 0.05 mL min<sup>-1</sup> flow rate of the polymer solution; 16 cm needle-to-collector distance. The electrospinning process was conducted at room temperature. The nanofibers were collected on an aluminum plate (15 × 15 cm) and dried, after overnight incubation at 30 °C for elimination of the residual solvent. Afterwards, the collected nanofibers were stored in light protected containers at room temperature.

#### 2.5. Antioxidant activity assays

The antioxidant activity of the nanofibers was evaluated by ABTS and DPPH radical scavenging assays, following procedures described by Mosayebi *et al.*,<sup>36</sup> with modifications. For ABTS assay, nanofibers (5 mg) were immersed in a 4 mL bicarbonate/carbonate buffer solution (0.2 M, pH 9.5), vortexed for 3 min and sonicated in a USC 700 ultrasonic bath (Unique, Americana, Brazil) for 15 min for proper hydrolysate extraction. Samples were centrifuged at 10 000g for 15 min, and an aliquot (100 μL) was mixed with 1 mL ABTS radical solution previously prepared according to Re *et al.*<sup>37</sup> After reacting in the dark for 6 min, absorbance was measured at 734 nm using a mini-1240 UV spectrophotometer (Shimadzu, Kyoto, Japan). A bicarbonate/carbonate buffer solution without nanofibers and mixed with ABTS radical solution was used as a control sample. The ABTS

free radical scavenging rate (%) was determined from the following equation:

$$\text{Antioxidant activity (\%)} = (A_{\text{control}} - A_{\text{sample}})/A_{\text{control}} \times 100 \quad (1)$$

where the absorbance values for the control sample (without nanofibers) and nanofiber sample are represented by  $A_{\text{control}}$  and  $A_{\text{sample}}$ , respectively. The results were also expressed as Trolox equivalent (TEAC) based on a standard curve of Trolox over a range of 0.1 to 2.0 mM.

DPPH scavenging activity was determined using the same procedure for FKH extraction from nanofibers. Then, 50 μL extracted sample was added into 1 mL radical DPPH solution (180 mM) freshly prepared in methanol. The samples were stirred in the vortex and incubated in the dark for 1 h at 25 °C. Absorbance was measured at 517 nm. For the control sample, a bicarbonate/carbonate buffer solution combined with the DPPH radical solution without nanofiber was prepared. The DPPH radical scavenging activity was calculated using the aforementioned eqn (1) and a specific TEAC for this radical.

#### 2.6. Characterization of nanofibers

**2.6.1. Scanning electron microscopy.** A Zeiss EVO 10 scanning electron microscope (Zeiss, Germany) was used for the morphological analysis of the electrospun nanofibers. Samples were coated with a 5 nm Au/Pd layer by sputtering and subsequently examined at an accelerating voltage of 10 kV.<sup>38</sup> After SEM image acquisition, the average fiber diameter (AFD) was determined by image analysis using the ImageJ software (National Institutes of Health, USA), in which 100 fibers for each treatment were randomly selected.

**2.6.2. Fourier transform infrared (FTIR) spectrometry.** For Fourier transform infrared (FTIR) characterization, samples were analyzed by using a Thermo Scientific Nicolet iN10 spectrometer (Thermo Fischer Scientific, USA) equipped with an Attenuated Total Reflection (ATR) unit with a diamond crystal. The scans were collected between 450 and 4000 cm<sup>-1</sup> at a 4 cm<sup>-1</sup> resolution.<sup>17</sup>

**2.6.3. Thermal analysis.** A thermogravimetric analyzer model TGA Pyris 1 (PerkinElmer, USA) was used for the thermal stability evaluation of PCL nanofibers. The samples were heated in platinum pans from 35 to 850 °C at the rate of 10 °C min<sup>-1</sup> under a nitrogen atmosphere (flow rate 20 mL min<sup>-1</sup>).<sup>39</sup> A differential scanning calorimeter DSC 8500 (PerkinElmer, USA) was used to analyze the thermodynamic behavior of the nanofiber films. Samples equivalent to approximately 11 mg were placed in aluminum pans and heated from 20 to 200 °C with a heating rate of 10 °C min<sup>-1</sup> under a nitrogen atmosphere. An empty pan sealed with a cover pan was used as a reference sample. Crystallinity for PCL nanofibers was calculated using the following equation:

$$\text{Crystallinity } (\chi_c) = \Delta H_m / \Delta H_c^\circ \quad (2)$$

where  $\Delta H_m$  is the enthalpy of fusion value found for each sample analyzed and  $\Delta H_c^\circ$  is the melting enthalpy of 100% crystalline PCL (81.6 J g<sup>-1</sup>) as described by Danesin *et al.*<sup>40</sup>



**2.6.4. Mechanical properties.** Tensile tests were carried out in order to determine the mechanical properties of nanofibers.<sup>41</sup> Samples of 0.1 mm thickness were cut into pieces of 50 × 10 mm and determination of elastic modulus (Young's modulus, MPa), tensile strength (MPa) and elongation at break (%) was carried out on a texture analyzer TA. XT Plus (Stable Micro Systems, Godalming, UK) using film geometry. In accordance with ASTM D638, a strain rate of 10 mm min<sup>-1</sup> and a clamping distance of 40 mm were used throughout the experiment. Tests were replicated at least three times for each sample.

## 2.7. Hemolysis assay

The hemolytic activity of nanofibers was evaluated using defibrinated sheep blood (NewProv, Pinhais, Brazil) as previously described.<sup>17</sup> Briefly, the erythrocytes were previously washed with 10 mM phosphate buffered saline (PBS; pH 7.4) solution followed by centrifugation at 900g, during 15 min at 4 °C. Nanofiber samples (4 mg) were suspended in 1 mL PBS and 1 mL erythrocyte suspension (4%; v/v) was added. After 60 min incubation at 37 °C, samples were centrifuged (3000g for 10 min) and the supernatant was collected. The released hemoglobin was determined by measuring the absorbance at 540 nm. Erythrocytes treated with 0.1% (v/v) Triton X-100 were used as a positive control (100% hemolysis). A PBS solution was used as a negative control. The following formula was employed in order to calculate the hemolytic activities:

$$\text{Hemolytic activity (\%)} = \frac{(A_{\text{sample}} - A_{\text{Negative}})}{(A_{\text{Positive}} - A_{\text{Negative}})} \times 100 \quad (3)$$

where  $A_{\text{sample}}$ ,  $A_{\text{Negative}}$  and  $A_{\text{Positive}}$  represent the absorbance values for the nanofiber samples, negative control and positive control, respectively.

## 2.8. In vitro FKH release assay

The release behavior of FKH loaded into PCL nanofibers was carried out by the migration test in simulant solutions. These solutions included ethanol 10% (v/v), ethanol 50% (v/v), and acetic acid 3% (v/v), which mimic the following different food categories: aqueous, fatty and acidic foods, respectively.<sup>42,43</sup> Aliquots were collected 72 h after nanofiber contact with the solutions in order to carry out the determination of soluble protein<sup>44</sup> as well as the DPPH radical scavenging activity.

## 2.9. Statistical analysis

All the tests were performed in triplicate and data were shown as mean ± standard deviation (SD) values. The results were subjected to analysis of variance (ANOVA) followed by Tukeys test using SAS for Windows ver. 9.0 (SAS Institute Inc., Cary, NC). Differences were considered significant for  $p$ -values < 0.05.

# 3 Results and discussion

## 3.1. Antioxidant activity of functionalized PCL nanofibers

The antioxidant properties of the PCL nanofibers functionalized with feather keratin hydrolysate (FKH) were evaluated by DPPH

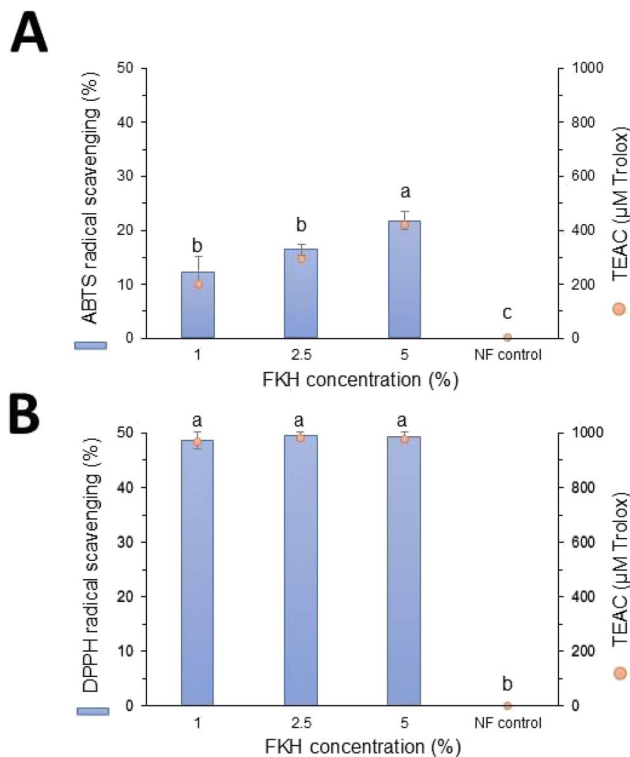


Fig. 1 Antioxidant activity of PCL nanofibers containing different concentrations of feather keratin hydrolysate (FKH) obtained from *Chryseobacterium* sp. kr6. Nanofibers without FKH were used as control (NF control). The samples were evaluated by ABTS (A) and DPPH (B) assays. The results are expressed as free radical scavenging percentage and their respective Trolox equivalent (TEAC). For each assay, different letters indicate a significant difference. Data were evaluated by ANOVA followed by Tukey's test ( $p < 0.05$ ). Data represent mean ± standard deviation of three independent experiments.

and ABTS radical scavenging assays. As shown in Fig. 1, FKH was successfully incorporated into PCL nanofibers since all samples presented antioxidant activity. These results suggest that the biological properties of FKH were preserved during the electrospinning process, in addition to being compatible with the polymer used for its incorporation. Nanofibers without the FKH did not present antioxidant activity (Fig. 1). The antioxidant capacity of FKH obtained by bacterial action was previously attributed to peptide LPGPILSSFPQ, in which its aromatic and hydrophobic amino acid residues are probably involved in free radical scavenging.<sup>10</sup>

It was also possible to observe a concentration-dependent capacity of the functionalized nanofibers on the scavenging properties against the ABTS radical (Fig. 1A). The highest antioxidant activity value was 21.58% (413.9 µM TEAC) for PCL nanofibers containing 5% FKH. This dose-dependent effect was not verified in the DPPH radical scavenging capacity assays (Fig. 1B). In this case, PCL nanofibers loaded with the three FKH concentrations exerted a similar profile on the DPPH radical scavenging, and no significant differences among the samples were observed. Furthermore, the antioxidant properties of these nanofibers against the DPPH radical were stronger than their ability to scavenge the ABTS radical, reaching values close to 50% (>950 µM TEAC).



The discrepancy between ABTS and DPPH results is an expected outcome due to the specific properties of each free radical, the antioxidant substance, and the reaction conditions, which may influence the results. The higher values obtained in DPPH assay even at lower concentrations of FKH could be related to the hydrophobic composition of keratin peptides,<sup>10</sup> which reacted more efficiently with DPPH radicals. Differences between the ABTS and DPPH radical scavenging activities were also verified in gelatin nanofibers functionalized with a spirulina protein concentrate, with values reaching 18% and 44% for DPPH and ABTS assays, respectively.<sup>36</sup>

### 3.2. Morphological characterization

The SEM images and histograms of fiber diameter distribution of electrospun PCL nanofibers prepared with different amounts of FKH (1, 2.5 and 5%) are displayed in Fig. 2. The addition of FKH to the PCL formulation did not cause notable morphological differences in relation to the bare PCL nanofibers. All samples showed a typical string-like morphology, continuous and uniform appearance, and without bead defects. However, the different FKH concentrations caused a gradual increase in the average nanofiber diameter. The control PCL nanofibers showed an average diameter of  $332 \pm 73$  nm, whereas the values for those containing 1, 2.5 and 5% FKH in the formulation were  $348 \pm 87$ ,  $363 \pm 70$  and  $533 \pm 167$  nm, respectively. The average diameter of the 5% FKH/PCL nanofibers was significantly higher ( $p < 0.05$ ) than that of the other nanofibers. A greater span of diameter distributions was also observed for the 5% FKH/PCL nanofibers.

Different studies have shown that certain compounds added to the polymeric solution can modify its viscosity, surface tension or conductivity, affecting the electrospinning process and, as a consequence, average nanofiber diameter.<sup>45–47</sup> A similar trend in increasing mean diameter was observed for PCL nanofibers functionalized with an antioxidant extract from *Ganoderma lucidum*.<sup>46</sup> According to the authors, higher extract

concentrations reduced the conductivity of the PCL solution, which allowed an increase in nanofiber diameter. On the other hand, a reduction in the average diameter of PCL nanofibers after adding quercetin in the spinning formulation was attributed to a decrease in its viscosity.<sup>47</sup> Therefore, the FKH addition possibly resulted in a modification in the polymeric solution viscosity and/or conductivity, providing lower stretching forces for the polymeric jet to form thicker fibers.

### 3.3. Infrared spectra

Infrared spectroscopy has been conducted to verify the interaction between the nanofiber components (FKH and PCL). The presence of FKH has no effect on the FTIR spectra of PCL nanofibers (Fig. 3). The infrared spectrum of control nanofibers is consistent with previous reports,<sup>17,35</sup> showing typical peaks of PCL such as prominent peaks at  $2941$  and  $2864$   $\text{cm}^{-1}$  (corresponding to asymmetric and symmetric  $\text{CH}_2$  stretching, respectively),  $1722$  and  $1293$   $\text{cm}^{-1}$  (attributed to carbonyl and C–C stretching, respectively),  $1238$  and  $1171$   $\text{cm}^{-1}$  (asymmetric and symmetric C–O–C stretching, respectively). The spectrum of PCL nanofibers also showed peaks at  $1108$  and  $1025$   $\text{cm}^{-1}$  both attributed to O–C vibrations.<sup>48</sup>

All nanofibers containing FKH presented similar FTIR spectra to the control sample with minor shifts. Characteristic peaks of FKH did not appear in the spectra of FKH/PCL nanofibers. In a previous study, the FTIR spectra of feather hydrolysate were found to be similar to those reported for keratins,<sup>11</sup> including the representative peaks at  $3424$   $\text{cm}^{-1}$  (N–H stretching vibration);  $2930$   $\text{cm}^{-1}$  (C–H stretching of the carbon backbone in peptides);  $1616$  and  $1402$   $\text{cm}^{-1}$  (amide I and amide II groups of proteins, respectively); and  $1118$   $\text{cm}^{-1}$  (amine group stretching vibration). The lack of significant differences in the functionalized nanofibers could be explained by some reasons such as the FKH amount in the analyzed sample was not sufficient to be detected or overlapping of some peaks with those referring to PCL. In the latter case, an amide group III

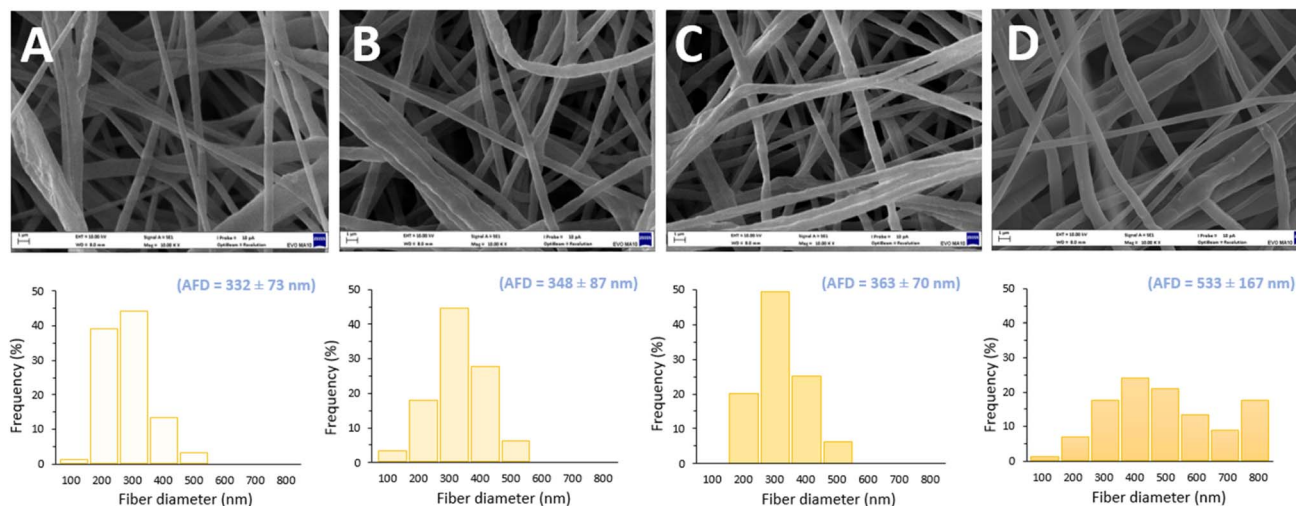


Fig. 2 SEM images (up) and fiber diameter distribution (down) of PCL nanofibers functionalized with feather keratin hydrolysate (FKH) at different concentrations: without (A), 1 (B), 2.5 (C) and 5% (D) FKH. Values immediately below the microscopy images (blue font) are the average fiber diameter (AFD)  $\pm$  standard deviation. Asterisk indicates significant differences by ANOVA and Tukey's test ( $p < 0.05$ ).



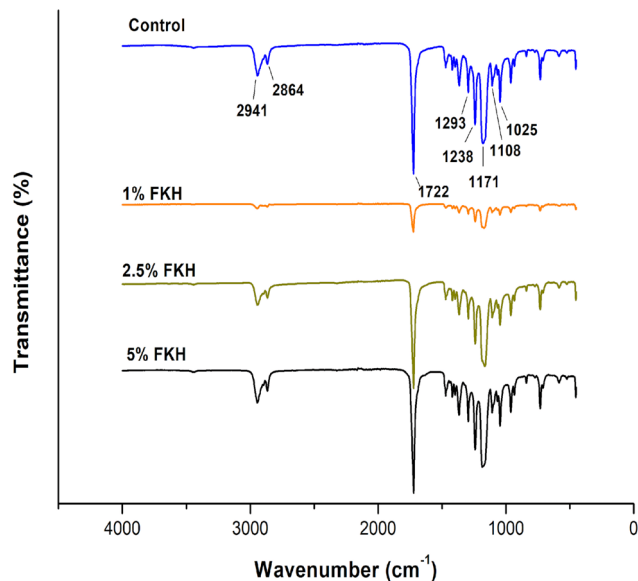


Fig. 3 Infrared spectroscopy analysis of PCL nanofibers functionalized with feather keratin hydrolysate (FKH) at different concentrations (1, 2.5 and 5% FKH) compared to PCL nanofiber control (without FKH).

absorption band, usually present at  $1232\text{ cm}^{-1}$  in keratin spectra<sup>49</sup> was probably overlapped by the peak at  $1238\text{ cm}^{-1}$  ascribed to the C–O–C stretching of PCL. Other typical peaks of FKH or keratin,<sup>48</sup> such as those found at  $2930$ ,  $1118$  and  $1025\text{ cm}^{-1}$ , may also have been overlapped by some of the previously mentioned PCL peaks. This fact still suggests FKH incorporation in the polymer matrix without affecting its structure, as reported by Raghunathan *et al.*<sup>50</sup> when similarities were found between the spectra of PCL nanofibers functionalized or not with a microalgal peptide.

### 3.4. Thermal properties

TGA analysis of the nanofibers provided information about their thermal stability when the samples were heated, as shown in Fig. 4 and ESI Table 1.<sup>†</sup> A single degradation step was observed for the control PCL nanofibers, in which the initial degradation temperature was recorded at  $350\text{ °C}$  and completed at  $481\text{ °C}$ , reaching a considerable weight decrease (98.3%). This was consistent with studies on the thermal behavior of this polymer.<sup>50,51</sup>

In general, the thermal performance of the FKH-functionalized nanofibers was maintained in this temperature range. A similar weight loss to the control sample was observed for nanofibers containing 1% FKH, probably due to the small amount added. In contrast, the addition of a higher amount of FKH in the polymeric solution slightly affected the thermal degradation behavior of nanofibers. For 2.5 and 5% FKH/PCL nanofibers, the maximum weight loss was 88 and 92%, respectively. Also, a second weight-loss stage occurred immediately after the first one, probably associated with carbonization of thermally resistant components of the FKH, causing degradation of the remaining mass (9.3 and 6.2%, for 2.5 and 5% FKH/PCL nanofibers, respectively).

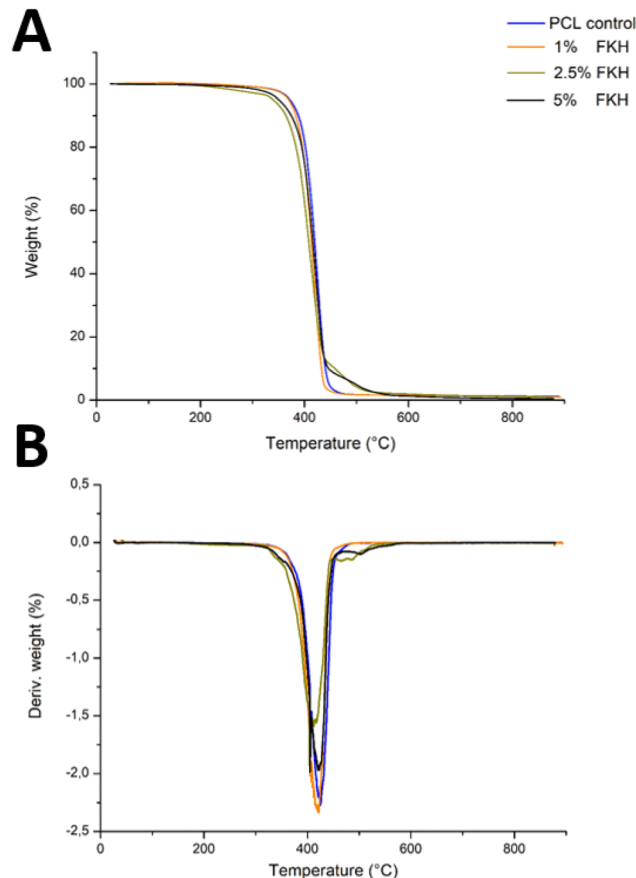


Fig. 4 Thermogravimetric analysis (A) and derivative curves (B) regarding weight loss of PCL nanofibers functionalized with feather keratin hydrolysate (FKH) at different concentrations (1, 2.5 and 5% FKH). Samples were compared to PCL nanofiber control (without FKH).

DSC thermograms of nanofibers are presented in ESI Fig. 1.<sup>†</sup> Control PCL nanofibers exhibited an endothermic fusion peak at  $58.9\text{ °C}$ , which corresponds to the polymer melting. This behavior was similar for nanofibers containing FKH, however, no specific melting peak for FKH was detected in the functionalized nanofibers, regardless of the concentration. Based on these observations, the hydrolysate could be present in the nanofibers as an amorphous state or dispersed in the polymer matrix.<sup>17,40</sup> DSC curves also allowed other parameters to be determined (Table 1), revealing the onset of melting temperature ( $T_{\text{onset}}$ ) and enthalpy of fusion ( $\Delta H_{\text{m}}$ ) at  $54.8\text{ °C}$  and  $71.7\text{ J g}^{-1}$ , respectively, for control nanofibers.  $T_{\text{onset}}$  and melting temperature values for the functionalized nanofibers were close to those from the control sample (approximately  $55$  and  $59\text{ °C}$ , respectively). Furthermore, measurements of  $\Delta H_{\text{m}}$  were slightly lower than the value calculated for the control nanofibers, but this did not affect the crystallinity of the samples. Danesin *et al.*,<sup>40</sup> verified some changes in the thermal parameters of PCL nanofibers when incorporating different synthetic peptides. The authors attributed this behavior to peptide interactions with both the PCL crystalline and amorphous states. This finding demonstrated that the incorporation of FKH did not cause critical effects on the thermal parameters of functionalized nanofibers.



**Table 1** Thermal parameters of different poly- $\epsilon$ -caprolactone (PCL) nanofibers derived from DSC thermograms. Nanofibers functionalized with feather keratin hydrolysate (FKH) at different concentrations (1, 2.5 and 5% FKH) were evaluated<sup>a</sup>

Sample	Thermal parameter			
	$T_{\text{onset}}$ (°C)	$T_m$ (°C)	$\Delta H_m$ (J g <sup>-1</sup> )	$X_c$
PCL control <sup>b</sup>	54.8 ± 0.1 <sup>a</sup>	58.9 ± 0.5 <sup>a</sup>	71.7 ± 0.6 <sup>a</sup>	0.87 ± 0.01 <sup>a</sup>
1% FKH/PCL	55.7 ± 0.4 <sup>a</sup>	59.9 ± 0.3 <sup>a</sup>	66.1 ± 0.1 <sup>b</sup>	0.81 ± 0.01 <sup>b,c</sup>
2.5% FKH/PCL	55.6 ± 0.2 <sup>a</sup>	58.5 ± 0.2 <sup>a</sup>	64.1 ± 0.3 <sup>b</sup>	0.78 ± 0.01 <sup>c</sup>
5% FKH/PCL	55.5 ± 0.3 <sup>a</sup>	59.5 ± 0.3 <sup>a</sup>	67.4 ± 0.3 <sup>b</sup>	0.82 ± 0.01 <sup>b</sup>

<sup>a</sup> Different letters in the same column indicate significant differences by ANOVA and Tukey's test ( $p < 0.05$ ). Data represent mean ± standard deviation of three independent experiments.  $T_{\text{onset}}$  = onset of the melting temperature;  $T_m$  = melting temperature;  $\Delta H_m$  = enthalpy of fusion;  $X_c$  = crystallinity, calculated as  $X_c = \Delta H_m / \Delta H_c^\circ$ , considering that the melting enthalpy of 100% crystalline PCL is 81.6 J g<sup>-1</sup>. <sup>b</sup> PCL nanofibers without addition of FKH.

### 3.5. Mechanical properties

The effects of FKH addition on the mechanical properties of the PCL electrospun nanofibers were investigated through the determination of the tensile strength ( $\sigma$ ), Young's modulus ( $E$ ) and elongation at break ( $\epsilon$ ). The tensile strength decreased in nanofibers containing FKH (Table 2), suggesting that the additive may cause a restriction in the segmental motions of neighboring polymer chains.<sup>52,53</sup> A reduction in this property can be attributed to the dispersion of the additive, since it may provide agglomerates and/or a greater interaction of FKH molecules, thus affecting the mechanical properties. In the case of elongation at break, the values were similar among pure PCL samples and samples with 2.5% FKH, while higher values were observed for nanofibers with 1 or 5% FKH (Table 2). The Young's modulus decreased from 40.6 MPa in the nanofibers without FKH to 16–18 MPa in nanofibers with 1 or 5% FKH, indicating a decrease in stiffness of the nanofiber mats.<sup>54</sup> Moreover, the alignment of the nanofiber at the time of deposition on the collector may also have been different among samples, resulting in a different conformation and changing the mechanical properties of the sample.<sup>55</sup>

### 3.6. Hemolytic activity

The potential of nanofibers to cause erythrocyte lysis was evaluated and the results are summarized in Fig. 5. As expected, the control PCL nanofibers did not substantially produce hemolysis

(around 1%). Similarly, the hemolytic degree of the nanofibers functionalized with FKH was also considered low. In this case, the hemolysis rates for PCL nanofibers containing 1, 2.5 and 5% FKH were 0, 1.6 and 3.0%, respectively. An elevated hemolysis rate may indicate the presence of reactive or toxic substances that harm blood cells and may have negative health implications.<sup>56</sup> In this regard, assays of hemolytic activity have been carried out to ensure the safety of packaging materials, especially those obtained from nanomaterials.<sup>57–60</sup> All these studies suggested a hemolysis threshold below 5% to indicate good compatibility and safety of the materials for food applications. However, further cytotoxicity studies are still needed to comprehensively ascertain the safety of these nanofibers.

### 3.7. FKH release

Nanofibers prepared from the highest concentration of FKH (5%) were selected and incubated in different simulant solutions in order to preliminarily evaluate their release capacity. FKH was released from PCL nanofibers for all proposed simulants since a gradual increase in protein concentration occurred after 6 h of contact of the nanofibers with these solutions (Fig. 6A). Furthermore, the DPPH scavenging activity was also

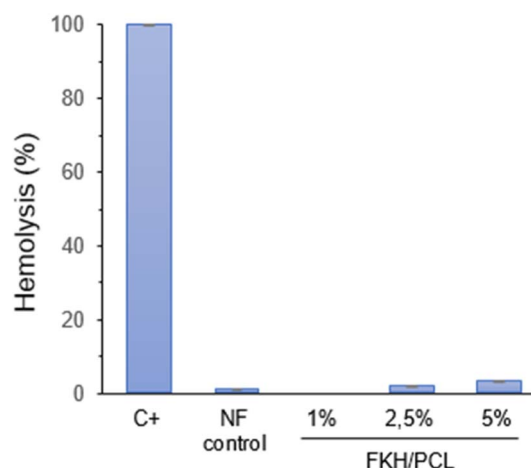


**Fig. 5** Hemolytic activity evaluation of PCL nanofibers functionalized with feather keratin hydrolysate (FKH) at different concentrations (1, 2.5 and 5% FKH) compared with PCL nanofibers without FKH (PCL control). Triton X-100 was used as positive control (C+) and was considered as 100% hemolysis. Results are the means ± standard deviations of three independent experiments.

**Table 2** Tensile properties of different poly- $\epsilon$ -caprolactone (PCL) nanofibers. Nanofibers functionalized with feather keratin hydrolysate (FKH) at different concentrations (1, 2.5 and 5% FKH) were evaluated<sup>a</sup>

Sample	Young's modulus (MPa)	Tensile strength (MPa)	Elongation at break (%)
PCL control	40.6 ± 5.7 <sup>a</sup>	5.7 ± 0.2 <sup>a</sup>	38.4 ± 2.9 <sup>b</sup>
1% FKH/PCL	16.5 ± 0.6 <sup>b</sup>	1.3 ± 0.1 <sup>c</sup>	118.2 ± 8.4 <sup>a</sup>
2.5% FKH/PCL	36.9 ± 3.6 <sup>a</sup>	2.9 ± 0.4 <sup>b</sup>	33.4 ± 6.9 <sup>b</sup>
5% FKH/PCL	18.2 ± 1.1 <sup>b</sup>	1.3 ± 0.1 <sup>c</sup>	112.7 ± 4.1 <sup>a</sup>

<sup>a</sup> Different letters in the same column indicate significant differences by ANOVA and Tukey's test ( $p < 0.05$ ). Data represent mean ± standard deviation of three independent experiments.



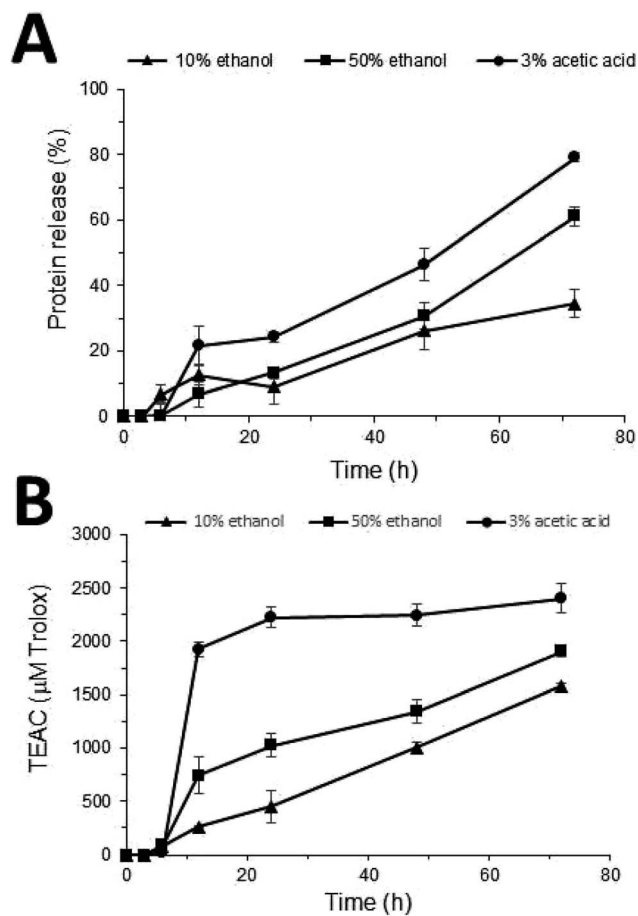


**Fig. 6** Release profile of feather keratin hydrolysate (FKH) at 5% from poly- $\epsilon$ -caprolactone nanofibers into food simulant solutions over 72 h incubation at 25 °C and 125 rpm. The samples were evaluated by protein determination (A) and DPPH (B) assays. The results are expressed as protein release percentage and Trolox equivalent (TEAC) for DPPH assays. Data represent mean  $\pm$  standard deviation of three independent experiments.

verified for the collected aliquots after this period (Fig. 6B). The acid food simulant promoted a significant ( $p < 0.05$ ) FKH release, in which approximately 80% of the original present in the nanofibers was released in 72 h. This behavior was also similar regarding the highest levels of antioxidant activity (2404  $\mu\text{M}$  TEAC) when compared to other solutions. These food simulants (hydrophilic, lipophilic, and acid) are commonly used to evaluate the release profile of active agents present in polymeric materials.<sup>17,43</sup> It is worth noting that proving the FKH controlled release capacity by nanofibers, including their evaluation in other simulating solutions, and the influence of different temperature conditions, are necessary steps for a more detailed study on the antioxidant potential of this material.

## 4 Conclusion

In this study, PCL nanofibers containing feather keratin hydrolysate (FKH) were successfully prepared and investigated for their antioxidant properties. The morphological and physicochemical characteristics of these nanofibers were not

significantly changed by the FKH addition in the polymeric solution as compared to control nanofibers. Antioxidant properties of the nanofibers were confirmed, highlighting those obtained with a higher concentration of FKH in their formulation (5% FKH/PCL). In addition to good antioxidant properties, these nanofibers did not show significant hemolysis indicating the biocompatible characteristics of this material. These results revealed the potential of the electrospinning technique as a suitable strategy for developing packaging materials incorporating bioactive hydrolysates. Likewise, obtaining antioxidant hydrolysates by microbial bioconversion of feathers could be an alternative for the recycling and valorization of poultry waste. Thus, innovative antioxidant nanofibers prepared from green treatment of feather waste were developed and characterized in this study. Additional steps towards cytotoxicity testing, biodegradation studies and evaluation in real food systems would enable their future use as an active material for the development of eco-friendly packaging.

## Data availability

The data supporting this article have been included in the main body or as part of the ESI.†

## Author contributions

FFV: conceptualization, formal analysis, validation, writing original draft. NJC: formal analysis, investigation, methodology. AAV: formal analysis, investigation, methodology. AB: conceptualization, funding acquisition, supervision, writing review & editing.

## Conflicts of interest

The authors declare no conflicts of interest.

## Acknowledgements

This work received financial support from Conselho Nacional de Desenvolvimento Científico e Tecnológico, CNPq [grant 308880/2021-8] and Fundação de Amparo à Pesquisa do Estado do Rio Grande do Sul, FAPERGS [grant 18/2551-000497-9]. The authors thank M.Sc. Diogo Vargas de Oliveira for technical support in electrospinning apparatus, Centro de Microscopia e Microanálise (CMM, UFRGS, Brazil) for technical support in electron microscopy and Laboratory of Physical Analysis (ICTA, UFRGS, Brazil) for technical support in thermal and mechanical analyses.

## References

- 1 A. Ferreira, S. S. Kunh, P. A. Cremonez, J. Dieter, J. G. Teleken, S. C. Sampaio and P. D. Kunh, Brazilian poultry activity waste: Destinations and energetic potential, *Renewable Sustainable Energy Rev.*, 2018, **81**, 3081–3089, DOI: [10.1016/j.rser.2017.08.078](https://doi.org/10.1016/j.rser.2017.08.078).



- 2 I. C. Ossai, F. S. Hamid and A. Hassan, Valorisation of keratinous wastes: A sustainable approach towards a circular economy, *Waste Manage.*, 2022, **151**, 81–104, DOI: [10.1016/j.wasman.2022.07.021](https://doi.org/10.1016/j.wasman.2022.07.021).
- 3 M. F. Ali, M. S. Hossain, T. S. Moin, S. Ahmed and A. M. S. Chowdhury, Utilization of waste chicken feather for the preparation of eco-friendly and sustainable composite, *Clean. Eng. Technol.*, 2021, **4**, 100190, DOI: [10.1016/j.clet.2021.100190](https://doi.org/10.1016/j.clet.2021.100190).
- 4 M. Kaur, A. K. Singh and A. Singh, Bioconversion of food industry waste to value added products: Current technological trends and prospects, *Food Biosci.*, 2023, **55**, 102935, DOI: [10.1016/j.fbio.2023.102935](https://doi.org/10.1016/j.fbio.2023.102935).
- 5 K. Callegaro, A. Brandelli and D. J. Daroit, Beyond plucking: Feathers bioprocessing into valuable protein hydrolysates, *Waste Manage.*, 2019, **95**, 399–415, DOI: [10.1016/j.wasman.2019.06.040](https://doi.org/10.1016/j.wasman.2019.06.040).
- 6 A. Jana, N. Kakkar, S. K. Halder, A. J. Das, T. Bhaskar, A. Ray, *et al.*, Efficient valorization of feather waste by *Bacillus cereus* IIPK35 for concomitant production of antioxidant keratin hydrolysate and milk-clotting metallo-serine keratinase, *J. Environ. Manage.*, 2022, **324**, 116380, DOI: [10.1016/j.jenvman.2022.116380](https://doi.org/10.1016/j.jenvman.2022.116380).
- 7 P. Kshetri, P. L. Singh, S. B. Chanu, T. S. Singh, C. Rajiv, K. Tamreihao, *et al.*, Biological activity of peptides isolated from feather keratin waste through microbial and enzymatic hydrolysis, *Electron. J. Biotechnol.*, 2022, **60**, 11–18, DOI: [10.1016/j.ejbt.2022.08.001](https://doi.org/10.1016/j.ejbt.2022.08.001).
- 8 A. Riffel, D. J. Daroit and A. Brandelli, Nutritional regulation of protease production by the feather-degrading bacterium *Chryseobacterium* sp. kr6, *New Biotechnol.*, 2011, **28**, 153–157, DOI: [10.1016/j.nbt.2010.09.008](https://doi.org/10.1016/j.nbt.2010.09.008).
- 9 R. Fontoura, D. J. Daroit, A. P. F. Correa, S. M. M. Meira, M. Mosquera and A. Brandelli, Production of feather hydrolysates with antioxidant, angiotensin-I converting enzyme- and dipeptidyl peptidase-IV-inhibitory activities, *New Biotechnol.*, 2014, **31**, 506–513, DOI: [10.1016/j.nbt.2014.07.002](https://doi.org/10.1016/j.nbt.2014.07.002).
- 10 R. Fontoura, D. J. Daroit, A. P. F. Correa, K. S. Moresco, L. Santi, W. O. B. Silva, *et al.*, Characterization of a novel antioxidant peptide from feather keratin hydrolysates, *New Biotechnol.*, 2019, **49**, 71–76, DOI: [10.1016/j.nbt.2018.09.003](https://doi.org/10.1016/j.nbt.2018.09.003).
- 11 D. Bertolini, M. E. P. Jiménez, C. dos Santos, A. P. F. Corrêa and A. Brandelli, Microbial bioconversion of feathers into antioxidant peptides and pigments and their liposome encapsulation, *Biotechnol. Lett.*, 2021, **43**, 835–844, DOI: [10.1007/s10529-020-03067-w](https://doi.org/10.1007/s10529-020-03067-w).
- 12 B. Preethi, N. Karmegam, S. Manikandan, S. Vickram, R. Subbaiya, S. Rajeshkumar, *et al.*, Nanotechnology-powered innovations for agricultural and food waste valorization: A critical appraisal in the context of circular economy implementation in developing nations, *Process Saf. Environ. Prot.*, 2024, **184**, 477–491, DOI: [10.1016/j.psep.2024.01.100](https://doi.org/10.1016/j.psep.2024.01.100).
- 13 A. B. Rashid, M. Haque, S. M. M. Islam and K. M. R. Uddin Labib, Nanotechnology-enhanced fiber-reinforced polymer composites: Recent advancements on processing techniques and applications, *Heliyon*, 2024, **10**, e24692, DOI: [10.1016/j.heliyon.2024.e24692](https://doi.org/10.1016/j.heliyon.2024.e24692).
- 14 M. A. Shah, T. Shahnaz, M. Zehab-ud-Din, J. H. Masoodi, S. Nazir, A. Qurashi, *et al.*, Application of nanotechnology in the agricultural and food processing industries: A review, *Sustainable Mater. Technol.*, 2024, **39**, e00809, DOI: [10.1016/j.susmat.2023.e00809](https://doi.org/10.1016/j.susmat.2023.e00809).
- 15 A. Hiwrale, S. Bharati, P. Pingale and A. Rajput, Nanofibers: A current era in drug delivery system, *Heliyon*, 2023, **9**, e18917, DOI: [10.1016/j.heliyon.2023.e18917](https://doi.org/10.1016/j.heliyon.2023.e18917).
- 16 M. Jurić, F. Donsi, L. M. Bandić and S. Jurić, Natural-based electrospun nanofibers: Challenges and potential applications in agri-food sector, *Food Biosci.*, 2023, **56**, 103372, DOI: [10.1016/j.fbio.2023.103372](https://doi.org/10.1016/j.fbio.2023.103372).
- 17 F. F. Veras, A. C. Ritter, I. Roggia, P. Pranke, C. N. Pereira and A. Brandelli, Natamycin-loaded electrospun poly( $\epsilon$ -caprolactone) nanofibers as an innovative platform for antifungal applications, *SN Appl. Sci.*, 2020, **2**, 1105, DOI: [10.1007/s42452-020-2912-z](https://doi.org/10.1007/s42452-020-2912-z).
- 18 S. Majidi, J. Movaffagh, H. Kamali, A. Shahroodi, M. Tafaghod and D. Salarbashi, Development and characterization of sumatriptan-loaded soy bean polysaccharide nanofiber using electrospinning technique, *J. Drug Delivery Sci. Technol.*, 2022, **78**, 103940, DOI: [10.1016/j.jddst.2022.103940](https://doi.org/10.1016/j.jddst.2022.103940).
- 19 Z. I. Yildiz, F. Topuz, M. E. Kilic, E. Durgun and T. Uyar, Encapsulation of antioxidant beta-carotene by cyclodextrin complex electrospun nanofibers: Solubilization and stabilization of beta-carotene by cyclodextrins, *Food Chem.*, 2023, 136284, DOI: [10.1016/j.foodchem.2023.136284](https://doi.org/10.1016/j.foodchem.2023.136284).
- 20 J. Yoon, J. Lee, S. P. Hong, H.-J. Park, J. Kim, J. Lee, *et al.*, Fabrication of biodegradable cellulose acetate nanofibers containing Rose Bengal dye by electrospinning technique and their antiviral efficacy under visible light irradiation, *Chemosphere*, 2024, **349**, 140897, DOI: [10.1016/j.chemosphere.2023.140897](https://doi.org/10.1016/j.chemosphere.2023.140897).
- 21 Y. Liu, X. Lan, J. Zhang, Y. Wang, F. Tian, Q. Li, *et al.*, Preparation and *in vitro* evaluation of  $\epsilon$ -poly(L-lysine) immobilized poly( $\epsilon$ -caprolactone) nanofiber membrane by polydopamine-assisted decoration as a potential wound dressing material, *Colloids Surf., B*, 2022, **220**, 112945, DOI: [10.1016/j.colsurfb.2022.112945](https://doi.org/10.1016/j.colsurfb.2022.112945).
- 22 F. B. Saripek, F. Sevgi and S. Dursun, Preparation of poly( $\epsilon$ -caprolactone) nanofibrous mats incorporating graphene oxide-silver nanoparticle hybrid composite by electrospinning method for potential antibacterial applications, *Colloids Surf., A*, 2022, **653**, 129969, DOI: [10.1016/j.colsurfa.2022.129969](https://doi.org/10.1016/j.colsurfa.2022.129969).
- 23 D. Murugan, A. Suresh, G. Thakur and B. N. Singh, Fabrication and evaluation of poly( $\epsilon$ -caprolactone) based nanofibrous scaffolds loaded with homoeopathic mother tincture of *Syzygium cumini* for wound healing applications, *OpenNano*, 2023, **14**, 100189, DOI: [10.1016/j.onano.2023.100189](https://doi.org/10.1016/j.onano.2023.100189).
- 24 M. Thakur, I. Majid, S. Hussain and V. Nanda, Poly( $\epsilon$ -caprolactone): A potential polymer for biodegradable food



- packaging applications, *Packag. Technol. Sci.*, 2021, **34**, 449–461, DOI: [10.1002/pts.2572](https://doi.org/10.1002/pts.2572).
- 25 D. Briassoulis, Agricultural plastics as a potential threat to food security, health, and environment through soil pollution by microplastics: Problem definition, *Sci. Total Environ.*, 2023, **892**, 164533, DOI: [10.1016/j.scitotenv.2023.164533](https://doi.org/10.1016/j.scitotenv.2023.164533).
- 26 J. E. Oney-Montalvo, D. A. Dzib-Cauich, E. d. J. Ramírez-Rivera, A. Cabal-Prieto and L. A. Can-Herrera, Applications of polycaprolactone in the food industry: A review, *Czech J. Food Sci.*, 2024, **42**(2), 77–84, DOI: [10.17221/200/2023-CJFS](https://doi.org/10.17221/200/2023-CJFS).
- 27 Z. Zheng, X. Dai, X. Li and C. Du, Functionalization of PCL-based nanofibers loaded with hirudin as blood contact materials, *Biomater. Adv.*, 2023, **149**, 213416, DOI: [10.1016/j.bioadv.2023.213416](https://doi.org/10.1016/j.bioadv.2023.213416).
- 28 Q. Li, W. Liang, L. Lv, Z. Fang, D. Xu, J. Liao, *et al.*, Preparation of PCL/lecithin/bacteriocin CAMT6 antimicrobial and antioxidant nanofiber films using emulsion electrospinning: Characteristics and application in chilled salmon preservation, *Food Res. Int.*, 2024, **175**, 113747, DOI: [10.1016/j.foodres.2023.113747](https://doi.org/10.1016/j.foodres.2023.113747).
- 29 S. S. Samavati, S. Kashanian, H. Derakhshankhah, R. A. Abuzade, S. Sajadimajd and M. Rabiei, PCL and PCL-Jaft nanofiber, synthesis, characterization, and histological comparison of the quality of wound healing, *J. Drug Delivery Sci. Technol.*, 2023, **84**, 104457, DOI: [10.1016/j.jddst.2023.104457](https://doi.org/10.1016/j.jddst.2023.104457).
- 30 T.-Y. Huang, J.-Y. Lin and W.-T. Su, Coaxial nanofibers encapsulated with *Ampelopsis brevipedunculata* extract and green synthesized AgNPs for wound repair, *Colloids Surf., B*, 2024, **235**, 113771, DOI: [10.1016/j.colsurfb.2024.113771](https://doi.org/10.1016/j.colsurfb.2024.113771).
- 31 G. Hu, Q. Huang, J. Li, Z. Wang, Y. Yu, W. Yang, *et al.*, PCL/Fucoidan nanofiber membrane loaded HP- $\beta$ -CD/EGC inclusion complexes for food packaging based on self-assembly strategy, *Food Hydrocolloids*, 2024, **151**, 109836, DOI: [10.1016/j.foodhyd.2024.109836](https://doi.org/10.1016/j.foodhyd.2024.109836).
- 32 L. Kuai, F. Liu, B.-S. Chiou, R. J. Avena-Bustillos, T. H. McHugh and F. Zhong, Controlled release of antioxidants from active food packaging: A review, *Food Hydrocolloids*, 2021, **120**, 106992, DOI: [10.1016/j.foodhyd.2021.106992](https://doi.org/10.1016/j.foodhyd.2021.106992).
- 33 F. Topuz and T. Uyar, Antioxidant, antibacterial and antifungal electrospun nanofibers for food packaging applications, *Food Res. Int.*, 2019, **130**, 108927, DOI: [10.1016/j.foodres.2019.108927](https://doi.org/10.1016/j.foodres.2019.108927).
- 34 A. Riffel, F. Lucas, P. Heeb and A. Brandelli, Characterization of a new keratinolytic bacterium that completely degrades native feather keratin, *Arch. Microbiol.*, 2003, **179**, 258–265, DOI: [10.1007/s00203-003-0525-8](https://doi.org/10.1007/s00203-003-0525-8).
- 35 F. F. Veras, I. Roggia, P. Pranke, C. N. Pereira and A. Brandelli, Inhibition of filamentous fungi by ketoconazole-functionalized electrospun nanofibers, *Eur. J. Pharm. Sci.*, 2016, **84**, 70–76, DOI: [10.1016/j.ejps.2016.01.014](https://doi.org/10.1016/j.ejps.2016.01.014).
- 36 V. Mosayebi, M. Fathi, M. Shahedi, N. Soltanzadeh and Z. Emam-Djomeh, Fast-dissolving antioxidant nanofibers based on Spirulina protein concentrate and gelatin developed using needleless electrospinning, *Food Biosci.*, 2022, **47**, 101759, DOI: [10.1016/j.fbio.2022.101759](https://doi.org/10.1016/j.fbio.2022.101759).
- 37 R. Re, N. Pellegrini, A. Proteggente, A. Panala, M. Yang and C. Rice-Evans, Antioxidant activity applying an improved ABTS radical cation decolorization assay, *Free Radical Biol. Med.*, 1999, **26**, 1231–1237, DOI: [10.1016/s0891-5849\(98\)00315-3](https://doi.org/10.1016/s0891-5849(98)00315-3).
- 38 M. F. Canbolat, A. Celebioglu and T. Uyara, Drug delivery system based on cyclodextrin–naproxen inclusion complexes incorporated in electrospun polycaprolactone nanofibers, *Colloids Surf., B*, 2014, **115**, 15–21, DOI: [10.1016/j.colsurfb.2013.11.021](https://doi.org/10.1016/j.colsurfb.2013.11.021).
- 39 Y. Ji, K. Liang, X. Shen and G. L. Bowlin, Electrospinning and characterization of chitin nanofibril/polycaprolactone nanocomposite fiber mats, *Carbohydr. Polym.*, 2014, **101**, 68–74, DOI: [10.1016/j.carbpol.2013.09.012](https://doi.org/10.1016/j.carbpol.2013.09.012).
- 40 R. Danesin, P. Brun, M. Roso, F. Delaunay, V. Samouillan, K. Brunelli, *et al.*, Self-assembling peptide-enriched electrospun polycaprolactone scaffolds promote the osteoblast adhesion and modulate differentiation-associated gene expression, *Bone*, 2012, **51**, 851–859, DOI: [10.1016/j.bone.2012.08.119](https://doi.org/10.1016/j.bone.2012.08.119).
- 41 S. Beikzadeh, S. M. Hosseini, V. Mofid, S. Ramezani, M. Ghorbani, A. Ehsani, *et al.*, Electrospun ethyl cellulose/poly caprolactone/gelatin nanofibers: The investigation of mechanical, antioxidant, and antifungal properties for food packaging, *Int. J. Biol. Macromol.*, 2021, **191**, 457–464, DOI: [10.1016/j.ijbiomac.2021.09.065](https://doi.org/10.1016/j.ijbiomac.2021.09.065).
- 42 European Commission, Commission regulation (EU) No 10/2011 on plastic materials and articles intended to come into contact with food, *Off. J. Eur. Union*, 2021, **12**, 1–87.
- 43 S. Estevez-Areco, S. Goyanes, M. C. Garrigós and A. Jiménez, Antioxidant water-resistant fish gelatin nanofibers: A comparative analysis of fructose and citric acid crosslinking and investigation of chlorogenic acid release kinetics, *Food Hydrocolloids*, 2024, **150**, 109696, DOI: [10.1016/j.foodhyd.2023.109696](https://doi.org/10.1016/j.foodhyd.2023.109696).
- 44 O. H. Lowry, N. J. Rosebrough, A. L. Farr and R. J. Randall, Protein measurement with the Folin phenol reagent, *J. Biol. Chem.*, 1951, **193**, 265–275.
- 45 X. Ji, R. Li, G. Liu, W. Jia, M. Sun, Y. Liu, *et al.*, Phase separation-based electrospun Janus nanofibers loaded with *Rana chensinensis* skin peptides/silver nanoparticles for wound healing, *Mater. Des.*, 2021, **207**, 109864, DOI: [10.1016/j.matdes.2021.109864](https://doi.org/10.1016/j.matdes.2021.109864).
- 46 S. Nabati, M. Aminzare, S. Roohinejad, H. H. Azar, M. Mohseni, R. Greiner, *et al.*, Electrospun polycaprolactone nanofiber containing *Ganoderma lucidum* extract to improve chemical and microbial stability of rainbow trout fillets during storage at 4 °C, *Food Control*, 2023, **150**, 109777, DOI: [10.1016/j.foodcont.2023.109777](https://doi.org/10.1016/j.foodcont.2023.109777).
- 47 Y. E. Bulbul and A. U. Oksuz, Cold atmospheric plasma modified polycaprolactone solution prior to electrospinning: A novel approach for improving quercetin-loaded nanofiber drug delivery systems, *Int. J. Pharm.*, 2024, **651**, 123789, DOI: [10.1016/j.ijpharm.2024.123789](https://doi.org/10.1016/j.ijpharm.2024.123789).



- 48 M. A. M. Hussein, E. Guler, E. Rayaman, M. E. Cam, A. Sahin, M. Grinholc, *et al.*, Dual-drug delivery of Ag-chitosan nanoparticles and phenytoin *via* core-shell PVA/PCL electrospun nanofibers, *Carbohydr. Polym.*, 2021, **270**, 118373, DOI: [10.1016/j.carbpol.2021.118373](https://doi.org/10.1016/j.carbpol.2021.118373).
- 49 S. Jung, B. Pant, M. Climans, G. C. Shaw, E.-J. Lee, N. Kim, *et al.*, Transformation of electrospun keratin/PVA nanofiber membranes into multilayered 3D scaffolds: Physicochemical studies and corneal implant applications, *Int. J. Pharm.*, 2021, **610**, 121228, DOI: [10.1016/j.ijpharm.2021.121228](https://doi.org/10.1016/j.ijpharm.2021.121228).
- 50 S. Raghunathan, S. Kandasamy, A. B. Pillai, D. P. Senthilathiban, N. Thajuddin, M. R. Kamli, *et al.*, Synthesis of biocomposites from microalgal peptide incorporated polycaprolactone/ $\kappa$ -carrageenan nanofibers and their antibacterial and wound healing property, *Int. J. Pharm.*, 2024, **655**, 124052, DOI: [10.1016/j.ijpharm.2024.124052](https://doi.org/10.1016/j.ijpharm.2024.124052).
- 51 T.-H. Kim, S.-C. Kim, W. S. Park, I.-W. Choi, H.-W. Kim, H. W. Kang, *et al.*, PCL/gelatin nanofibers incorporated with starfish polydeoxyribonucleotides for potential wound healing applications, *Mater. Des.*, 2023, **229**, 111912, DOI: [10.1016/j.matdes.2023.111912](https://doi.org/10.1016/j.matdes.2023.111912).
- 52 J. DeFelice and J. E. G. Lipson, The influence of additives on polymer matrix mobility and the glass transition, *Soft Matter*, 2021, **17**, 376–387, DOI: [10.1039/D0SM01634A](https://doi.org/10.1039/D0SM01634A).
- 53 B. D. Ippel, E. E. Van Haften, C. V. C. Bouten and P. Y. W. Dankers, Impact of additives on mechanical properties of supramolecular electrospun scaffolds, *ACS Appl. Polym. Mater.*, 2020, **2**, 3742–3748, DOI: [10.1021/acsapm.0c00658](https://doi.org/10.1021/acsapm.0c00658).
- 54 Z. Katančić, J. Travaš-Sejdić and Z. Zlata Hrnjak-Murđić, Study of flammability and thermal properties of high-impact polystyrene nanocomposites, *Polym. Degrad. Stab.*, 2011, **96**, 2104–2111, DOI: [10.1016/j.polyimdeggradstab.2021.09.020](https://doi.org/10.1016/j.polyimdeggradstab.2021.09.020).
- 55 G. Zehetmeyer, S. M. M. Meira, J. M. Scheibel, C. B. Silva, F. S. Rodembusch, A. Brandelli, *et al.*, Biodegradable and antimicrobial films based on poly(butylene adipate-co-terephthalate) electrospun fibers, *Polym. Bull.*, 2017, **74**, 3243–3268, DOI: [10.1007/s00289-016-1896-8](https://doi.org/10.1007/s00289-016-1896-8).
- 56 Y. Tian, Z. Tian, Y. Dong, X. Wang and L. Zhan, Current advances in nanomaterials affecting morphology, structure, and function of erythrocytes, *RSC Adv.*, 2021, **11**, 6958–6971, DOI: [10.1039/d0ra10124a](https://doi.org/10.1039/d0ra10124a).
- 57 Y. Ni, S. Shi, M. Li, L. Zhang, C. Yang and T. Du, Visible light responsive, self-activated bionanocomposite films with sustained antimicrobial activity for food packaging, *Food Chem.*, 2021, **362**, 130201, DOI: [10.1016/j.foodchem.2021.130201](https://doi.org/10.1016/j.foodchem.2021.130201).
- 58 K. Ma, T. Zhe, F. Li, Y. Zhang, M. Yu, R. Li, *et al.*, Sustainable films containing AIE-active berberine-based nanoparticles: A promising antibacterial food packaging, *Food Hydrocolloids*, 2022, **123**, 107147, DOI: [10.1016/j.foodhyd.2021.107147](https://doi.org/10.1016/j.foodhyd.2021.107147).
- 59 M. H. Al-Musawi, A. Khoshkalampour, H. A. S. Al-Naymi, Z. F. Shafeeq, S. P. Doust and M. Ghorbani, Optimization and characterization of carrageenan/gelatin-based nanogel containing ginger essential oil enriched electrospun ethyl cellulose/casein nanofibers, *Int. J. Biol. Macromol.*, 2023, **248**, 125969, DOI: [10.1016/j.ijbiomac.2023.125969](https://doi.org/10.1016/j.ijbiomac.2023.125969).
- 60 L. Zhang, P. Hu, W. He, W. Wang, L. Luo, Q. Li, *et al.*, Mild temperature-assisted antimicrobial film with self-activating biocatalytic activity for efficient preservation of perishable products, *Food Hydrocolloids*, 2024, **146**, 109278, DOI: [10.1016/j.foodhyd.2023.109278](https://doi.org/10.1016/j.foodhyd.2023.109278).

